A METHODOLOGY FOR ESTIMATING DURABILITY OF AM50 MAGNESIUM ALLOY STEERING WHEELS

LIVIU MARŞAVINA, TAMÁS KRAUSZ, LIVIU PÎRVULESCU, LUCIAN RUSU

Abstract. Magnesium alloys have been widely spread in the automotive industry by their advantage: good mechanical properties, lightweight structure thanks to magnesium's low density. This paper proposes a methodology to estimate durability of a magnesium alloy AM50 steering wheel. The methodology is based on experimentally determined mechanical and fatigue properties and numerical simulation. The methodology was validated for two types of specimens against experimental fatigue data, and then applied to a steering wheel under torsion, respectively bending loading.

Keywords: magnesium alloy, stress concentration, durability.

1. INTRODUCTION

Automotive industry is one of the most developed industries, especially nowadays when car producers have to go hand by hand with the high-end technologies in order to be marketable and to offer something more than their competitors do. Besides electronics, materials also play a very important role in the successful development of new cars and components. The continuous search for light, but durable materials determined the usage of magnesium alloys, this type of material assuring low weight and relatively good mechanical properties [1].

Magnesium alloys are good alternatives for the parts of an automobile, however the selection of these alloys requires to know the mechanical properties of every specific alloy and their limitations [2]. The intention to use magnesium alloys for crash sensitive components necessitates the characterization of the different alloys by their mechanical parameters under static and dynamic loading and the study of their deformation behavior [3].

Fatigue properties of different magnesium alloys, obtained by die casting or extruding, were experimentally determined in high cycle fatigue: AM60 [4–6], AM20 and AM50 [7], NZ series [8–9] and AZ series [10–16], in order to determine the fatigue properties using rotating bending, axial tension-compression and

University Politehnica of Timisoara, Faculty of Mechanical Engineering, Romania

multiaxial tension-torsion tests. Low cycle fatigue tests were carried out on axial loading on different materials like: AM50 [17,18], AM60 [19], AZ31 [20-23], AZ80 [24], GW series [25].

Mechanical properties of the magnesium alloys are highly influenced by the manufacturing processes [3]. Die-cast products, in many cases, present a variety of casting defects such as cracks, porosity, oxide films, intermetallic particles, defects which are harmful to the mechanical properties, including fatigue behavior (Fig.1).

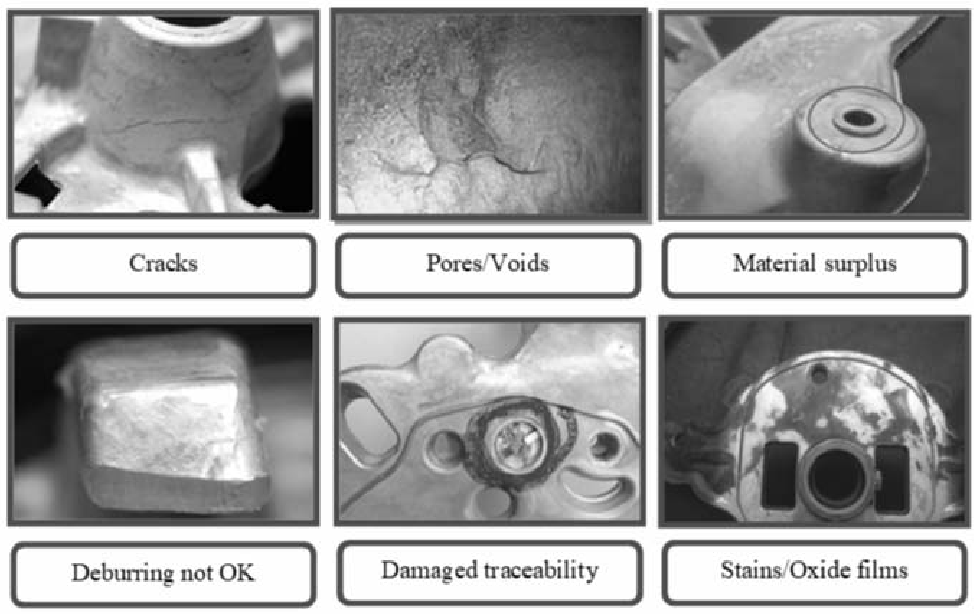

Fig. 1 – Common defects for die-casted magnesium alloys.

Another important aspect, which should be taken into account when designing magnesium alloy components, besides the defects that could affect the injected parts, is the effect of stress concentrators and surface finishing.

This paper proposes a methodology to estimate durability of magnesium alloy components based on experimental static and fatigue data and finite element method.

2. EXPERIMENTAL DATA

The AM50 specimens used for static and fatigue tests, were die-casted in the same conditions (injection parameters, temperature, humidity etc.) as the steering wheels, in a specially designed injection mold for specimens.

Table 1 presents the chemical composition for the AM50 alloy specimens.

Table 1

Chemical composition of the investigated AM50 alloy

Material	Aluminum [%]	Manganese [%]	Zinc [%]	Iron [%]	Nickel [%]
AM50	4.90	0.32	0.22	Max. 0.004	Max. 0.002

2.1. Static tests

Prior to fatigue tests, static tensile tests were performed on cylindrical specimens with ϕ 6.5 mm diameter in the calibrated area. All the tests were carried out on raw test specimens, without any kind of machining of the exterior surfaces.

Tests were performed on a servo-hydraulic testing machine Instron 8874 (with maximum load 25 kN), at room temperature (23° C, humidity 50%), with a loading speed of 1 mm/min [26] – Fig. 2. The strains were recorded using a video-extensometer. Tensile tests were carried out according to ASTM B 557M – 02 [27], correspondingly the yield stress was determined at 0.2% strain. Typical engineering stress – engineering strain curve from tensile tests is shown in Fig. 3. The mean values of the mechanical properties for AM50 in tension: elastic modulus (E), yield strength ($R_{p0.2}$), tensile strength (R_M) and strain (ε) at break are presented in Table 2, together with results from literature [17]. They are in a good agreement for the yield stress (1.8% smaller), for the tensile strength (3% higher), respectively the strain at break (lower with 3.3%).

From Fig. 3 a non-linear behavior of AM50 magnesium alloy can be observed, described as a linear elastic part followed by a hardening domain. The static behavior in tensile of AM50 was modelled considering three different material models: linear elastic-plastic, Johnson-Cook, respectively Ramberg-Osgood. The linear elastic model with isotropic plasticity and the Johnson-Cook hardening model provide the best predictions of the AM50 behavior [26].

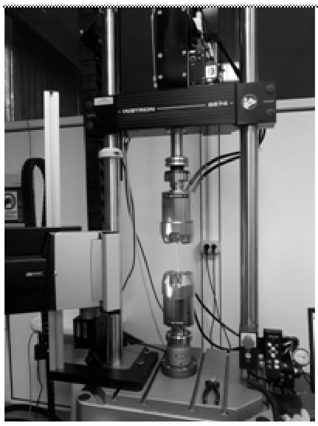

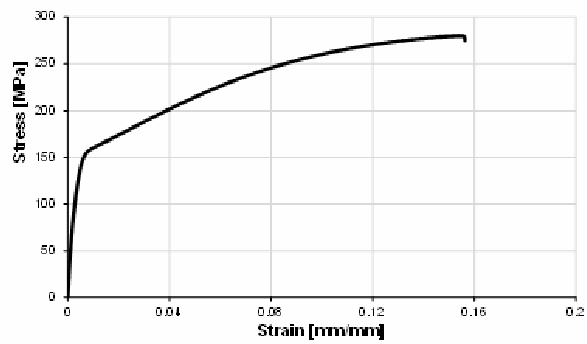

Fig. 2 — INSTRON testing machine. Fig. 3 — Typical engineering stress – strain curve.

Table 2

Tensile properties of the investigated Mg alloy

Material	Young's modulus [MPa]	Poisson's ratio [–]	Tensile strength [MPa]	Yield stress [MPa]	Strain at break [%]
AM50 from tests	45 870	0.385	236.9	122.8	14.5
AM50 from [16]	45 000	–	230	125	15

2.2. Fatigue tests

A detailed report on the fatigue test results of AM50 magnesium alloy is presented in Marsavina et al. [28]. In this paper, only some of the results are reviewed in order to validate the numerical methodology to predict the durability of AM50 components.

The specific standards from automotive industry prescribe for steering wheels a durability in the range of $2\cdot 10^5$ and $4\cdot 10^5$ cycles, corresponding to medium cycle fatigue. In consequence, the experimental fatigue tests have been performed up to 10^6 cycles.

The rotating bending tests were carried out for fatigue properties determination using a fully reversed cycle with coefficient $R=\frac{\sigma_{min}}{\sigma_{max}}=-1$. Tests were performed on a Wöhler type test equipment, presented in Fig. 4, at a frequency of 45 Hz and at room temperature conditions.

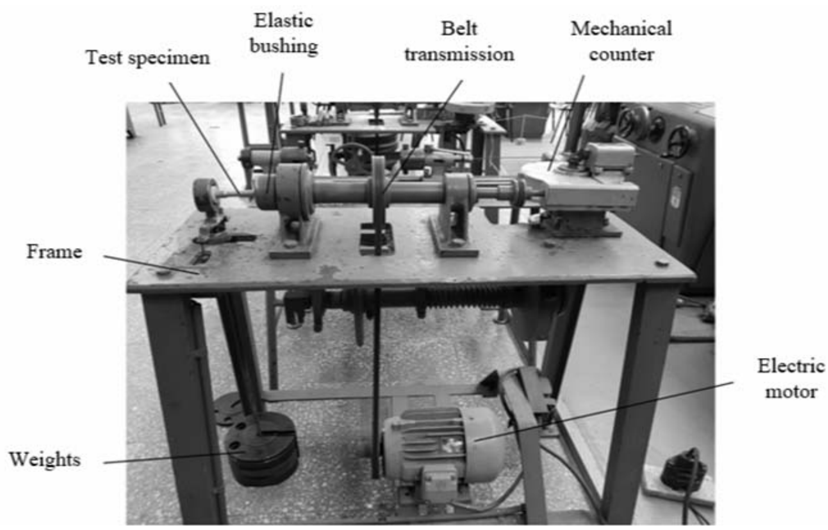

Fig. 4 – Wöhler type fatigue test equipment under rotating bending load condition.

Because steering wheel frames are structures with several stress concentrators, three types of specimens have been considered for the fatigue tests:

– as casted with a radius R_a = 10 mm, without surface finishing, having ϕ 12 mm diameter in the calibrated region and a radius of 10 mm to the gripping ends (Fig. 5a);

– un-notched, having a surface finishing obtained by turning to ϕ10 mm in the smallest cross section (Fig. 5b);

– notched with a 60° V-notch on a depth of 1 mm per radius (Fig. 5c).

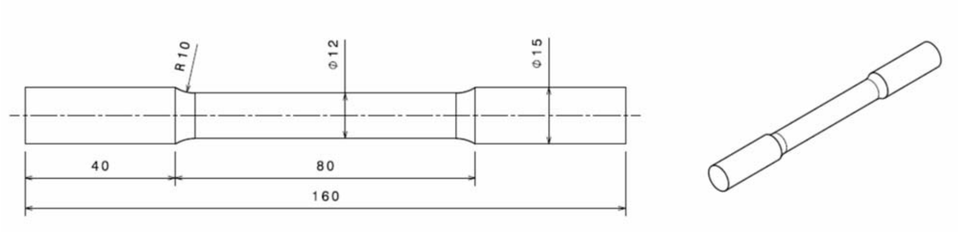

a. Specimen with radius R_a=10 mm as casted

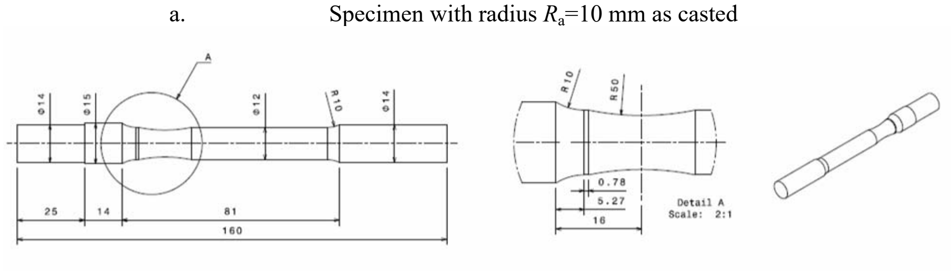

b. Specimen un-notched with calibration finish

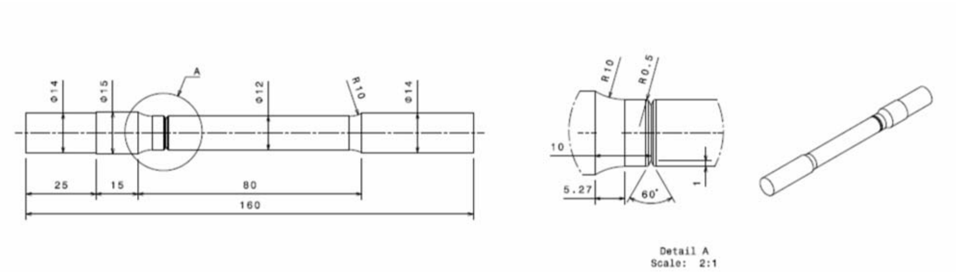

c. Specimen with V-notch

Fig. 5 – Specimens used for rotating bending fatigue tests.

At each load level, three specimens have been tested. If the specimen did not fail, after 10^6 cycles the test was stopped.

The fatigue test results for each specimen type are reported in Marsavina et al. [28].

3. NUMERICAL ESTIMATION OF DURABILITY

For numerical simulation of fatigue tests the geometries of the tested specimens were modeled in *Catia V5* design software and imported in the finite element simulation software *ANSYS Workbench*. The two CAD models have been meshed with SOLID187 type elements, resulting in 150 444 number of elements with 258 820 number of nodes, for the un-notched specimen, and in 236 799 number of elements and 395 809 number of nodes for the V-notched specimen (Fig. 6). A convergence study was performed under static loading conditions.

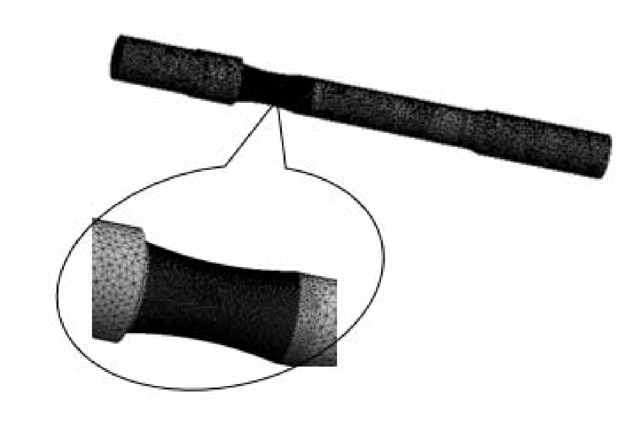

a. Un-notched specimen

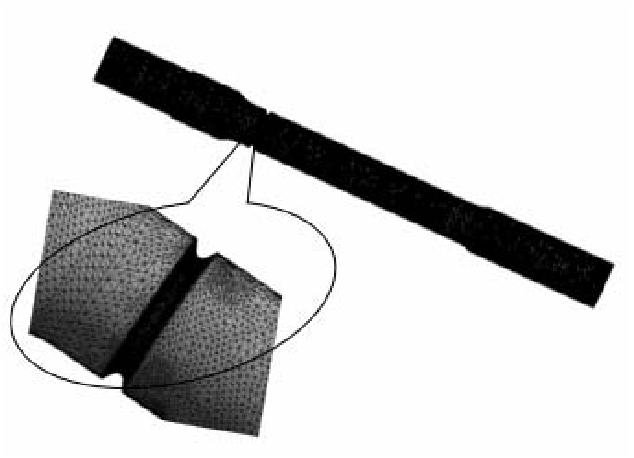

b. V-notched specimen

Fig. 6 – Meshing of the specimens.

The static results were used to calculate the stress concentration factor, which results in 1.05 for the un-notched specimen and *R*-radius specimen, respectively 2.58 for the V-notched specimen.

The elastic material properties have been defined according to the static tests results as the following: modulus of elasticity, E = 45.87 GPa, Poisson's ratio, $\nu = 0.385$, (Table 2). The fatigue curve was considered from the specimen with radius R_a=10 mm, as presented in Fig. 7. Statistical analysis was performed on fatigue data and the fatigue curve was obtained in the form:

$$\sigma_a = \sigma_{f'} \left(N_f\right)^b, \quad (1)$$

with $\sigma_{f'} = 419.31\text{MPa}$ and $b = -0.167$.

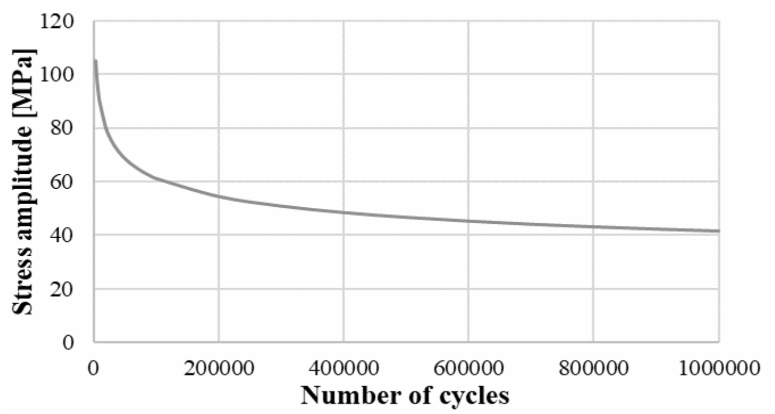

Fig. 7 – Fatigue curve for AM50 specimen with no stress concentration factor (specimen with radius R_a).

Boundary conditions were imposed by blocking the displacement of one of the ends of the test specimen, similar to its fixation in the testing equipment, and by applying different values of a load, corresponding to the forces applied during the fatigue tests, on the other end of the specimen (Fig. 8). Simulations have been performed up to force levels corresponding to a durability of 10^6 cycles (fatigue life of steering wheels is recommended to be between $2 \cdot 10^5 - 4 \cdot 10^5$ cycles).

The durability estimation of the specimens was carried out by using *ANSYS Workbench's Fatigue Tool*. The loading cycle has been considered as fully reversed, having an asymmetry coefficient of $R = -1$, mean stress $\sigma_{med} = 0$ and a correction factor of the fatigue strength $K_f = 1$, taking into account that the notched specimens were manufactured in the same injection conditions and have the same dimensions as the un-notched specimens for which the fatigue curve has been previously determined. The obtained fatigue results for a particular load are presented in Fig. 9.

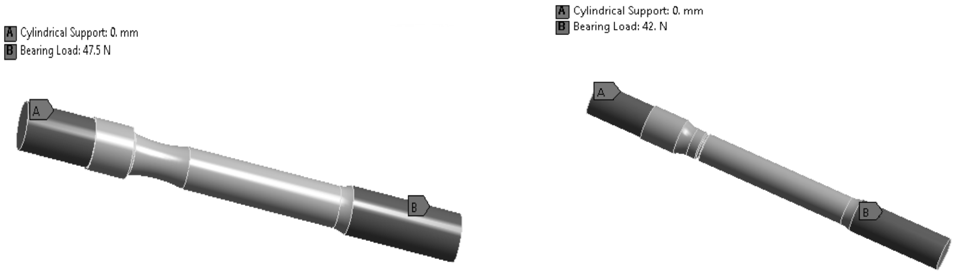

a. Specimen with U-shape notch b. Specimen with V-shape notch

Fig. 8 – Imposed boundary conditions.

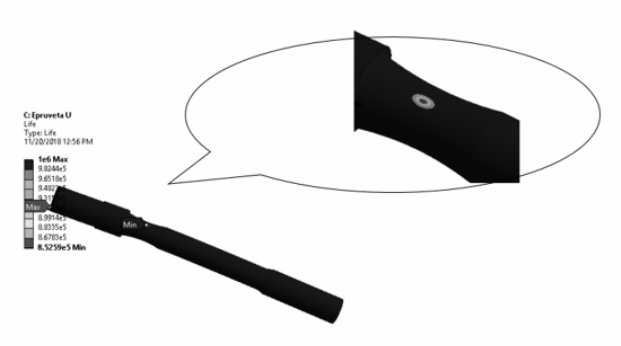

a. Specimen with U-notch (F = 47.5 N)

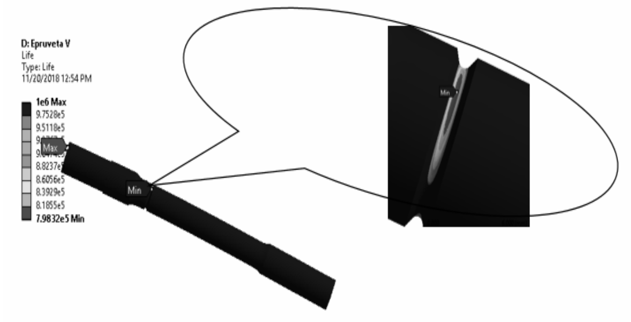

b. Specimen with V-notch (F = 42 N)

Fig. 9 – Durability of test specimens resulted from finite element analysis.

From the simulations, as we expect, it can be observed that the durability of the un-notched specimen (852 590 cycles) is greater than in the case of the V-shaped specimen (798 324 cycles), even if the load is 13% higher in the case of un-notched specimen. This difference highlights the effect of decreasing durability due to the increasing the stress concentrator. Different levels of load were considered, similar to those from the experiments. Figure 10 presents a comparison of experimental result to numerical prediction of the durability, expressed in terms of stress amplitude *versus* number of cycles for the rotating bending fatigue tests. By analyzing the curves, a good correlation can be observed. For the un-notched specimens, the estimated durability is inferior compared to the experimentally determined fatigue strength, showing a conservative numerical simulation.

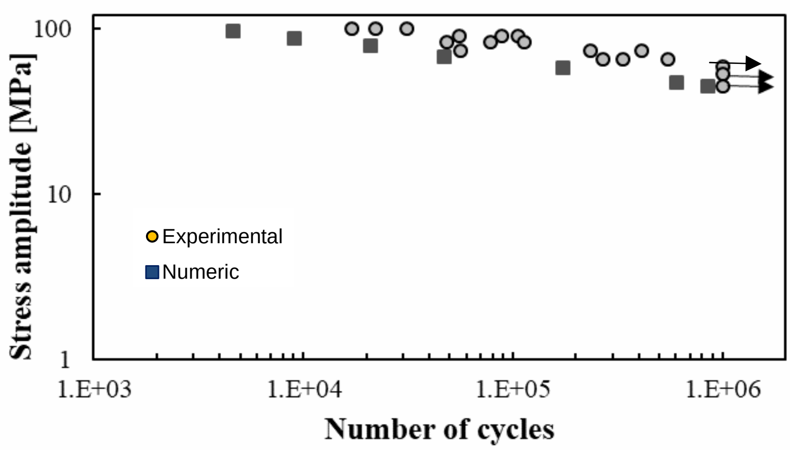

a. un-notched specimen

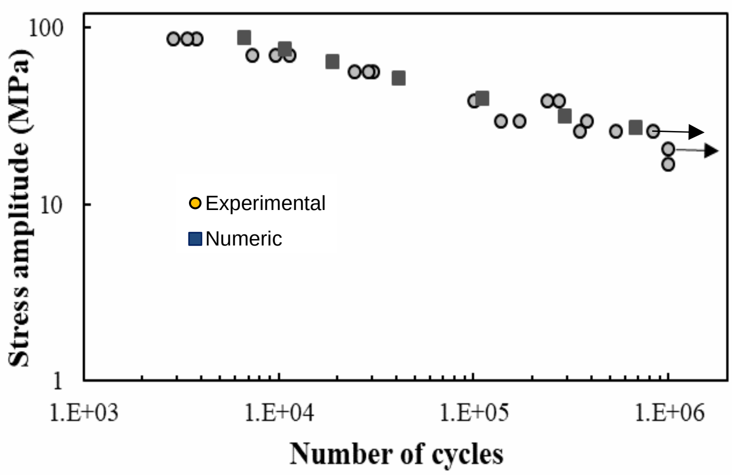

b. V-shape notched specimen

Fig. 10 – Comparison between experimental and numerical results for un-notched and notched test specimens.

4. ESTIMATION OF DURABILITY FOR A STEERING WHEEL

For estimating the durability of a steering wheel, we proposed the methodology presented in Fig. 11.

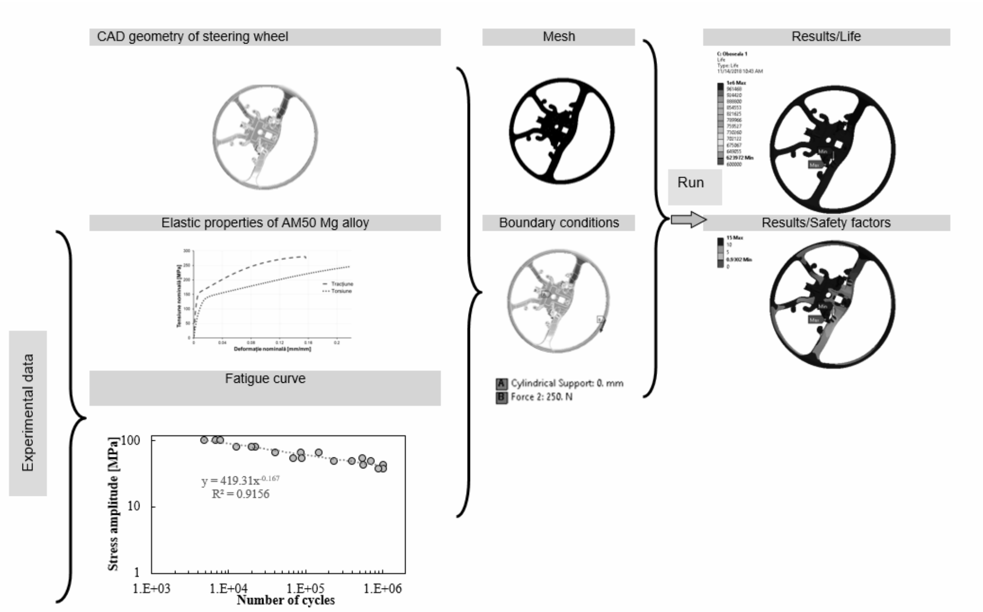

Fig. 11 – Methodology for evaluating durability of steering wheels.

The first step of applying the methodology is to prepare the 3D model of the steering wheel that needs to be evaluated. After preparing and importing the steering wheel model in the simulation software the next step is to define the mechanical properties as follows: elasticity modulus, Poisson's ratio, yield strength, ultimate strength and the stress–strain curve, obtained by performing static tensile tests. The fatigue curve obtained from the rotating bending fatigue tests should also be defined.

The 3D geometry needs to be meshed and boundary conditions have to be defined, in accordance with the steering wheel testing norms [29]. Basically, two types of tests are required for qualification: bending and torsion tests.

The initial results obtained in the simulations are the deformations, stresses and strains, after which, by using the *Fatigue Tool* of *ANSYS Workbench* version 18.2, durability estimation can be calculated, in addition to the safety factors across the model.

The geometric model from Fig. 12 was imported and then meshed in 511 467 SOLID187 elements (Fig. 13), connected in 888 580 nodes. The imposed elastic and fatigue properties where those obtained experimentally and presented above.

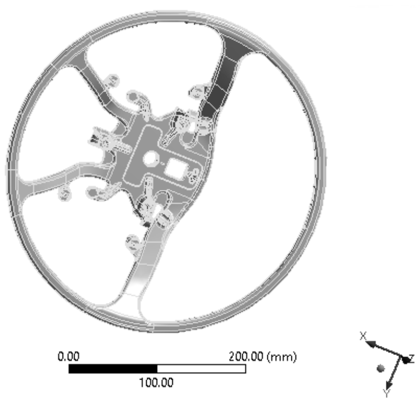

Fig. 12 – Steering wheel geometry.

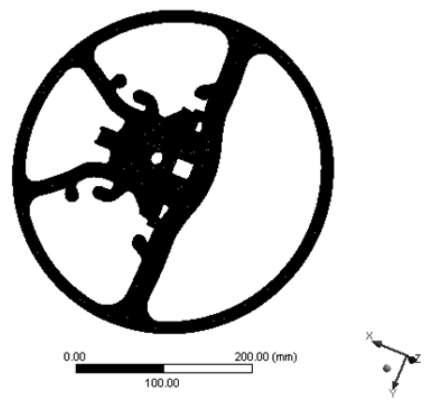

Fig. 13 – The mesh of the model.

Two scenarios were considered for loading the steering wheel, according to the fatigue tests [29]: a torsion load of the steering wheel with a tangential force of 250 N (Fig. 14a), respectively a bending load with a vertical force of 300 N applied to the steering wheel in the operating position (Fig. 14b). For both cases a cylindrical support was imposed on the splined mounting area of the steering wheel.

Depending on car producer, the prescribed durability of steering wheel is between 200 000 and 400 000 cycles.

a. torsion of steering wheel b. bending of steering wheel

Fig. 14 – Boundary conditions.

The static analysis of the steering wheel provides the total displacements Fig. 15 and the Von Mises equivalent stresses (Fig. 16). The maximum total displacement was obtained for bending of steering wheel 6.7 mm. The maximum equivalent stresses (Von Mises) were 93.16 MPa for torsion loading, respectively 99.5 MPa for bending load, both below the yield stress of the AM50 magnesium alloy (122.8 MPa, Table 2). This also confirms that the fatigue loadings are in the elastic regime.

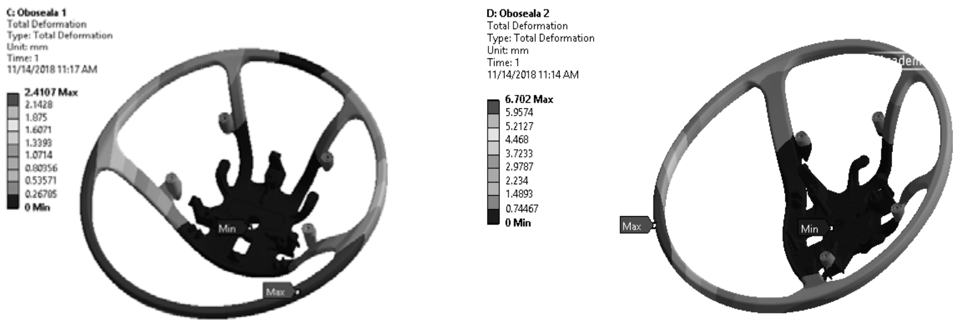

a. torsion of steering wheel b. bending of steering wheel

Fig. 15 – Total displacement.

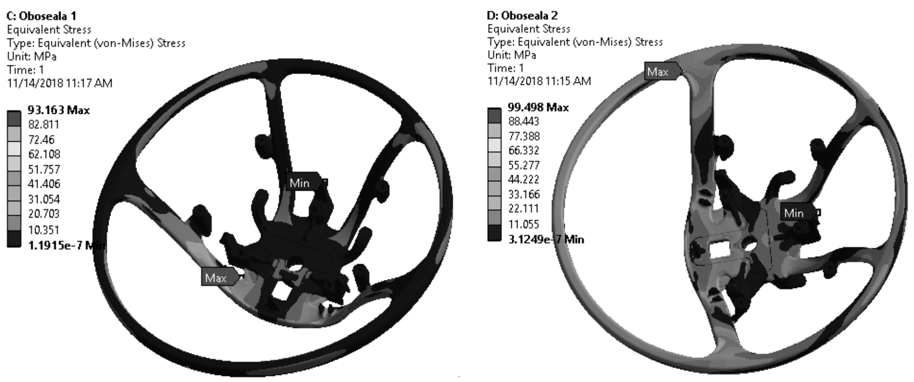

a. torsion of steering wheel b. bending of steering wheel

Fig. 16 – Von Mises equivalent stress.

The *Fatigue Tool* module was employed for durability calculations. A fully reversed $\left(R = \frac{\sigma_{\min}}{\sigma_{\max}} = -1 \right)$ cycle was defined with the same maximum loads as those used for static calculations. Also, a fatigue coefficient $K_f = 1$, taking into account that the fatigue curve was determined on specimens manufactured with the same casting conditions like the steering wheels, and no mean stress effect was considered. Figure 17 presents the durability of the steering wheel for the two loading scenarios. It could be observed that the minimum durability is 623 972 cycles in torsion, respectively 411 803 cycles in bending, both are above the minimum prescribed durability for this type of steering wheel of $3 \cdot 10^5$ cycles.

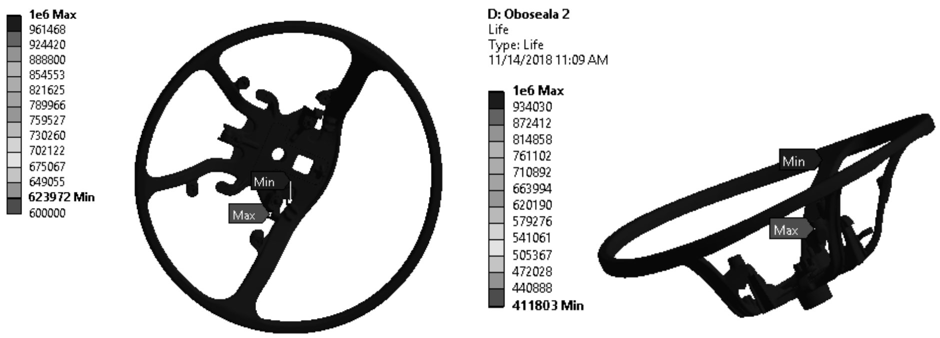

a. torsion of steering wheel b. bending of steering wheel

Fig. 17 – Steering wheel durability.

The minimum values of durability were obtained in the fillet radius between plateau and spoke for torsion test, respectively crown and spoke for bending test.

The proposed methodology of predicting the steering wheels' durability can save many hours of fatigue testing of steering wheels.

5. CONCLUSIONS

The paper proposed a numerical methodology to estimate durability of steering wheels.

The mechanical and fatigue properties of the AM50 magnesium alloy were determined by tensile tests, respectively rotating bending fatigue tests. These properties were used in the numerical prediction of durability.

The methodology was validated for two types of specimens (un – notched and V-notched), and then applied to a steering wheel.

Finally, the proposed methodology for durability estimation can be very helpful in the design process for steering wheel manufacturers, saving time and cost efforts by replacing the experimental fatigue tests.

Acknowledgements. This research was supported by the UEFISCDI Romania under a Bridge Grant program, contract number BG89/2016.

Received on August 1, 2019

REFERENCES

1. LUO A. A., *Magnesium casting technology for structural applications*, Journal of Magnesium and Alloys, **1**, *1*, pp. 2–22, 2013.
2. FRIEDRICH H., SCHUMANN S., *Research for a "new age of magnesium" in automotive industry*, J. Mater. Proc. Technol., **117**, pp. 276–281, 2001.
3. FRIEDRICH H.E., MORDIKE B.L. *Magnesium Technology–Metallurgy, Design Data, Applications*, Springer, 93, 2006.
4. LU Y., TAHERI F., GHARGHOURI M.A., HAN H.P., *Experimental and numerical study of the effects of porosity on fatigue crack initiation of HPDC magnesium AM60B alloy*, J Alloy Compd, **470**, *1-2*, pp. 202–213, 2008.
5. HORSTEMEYER M.F., YANG N., GALL K., MCDOWELL D., FAN J., GULLET P.M., *High cycle fatigue mechanisms in a cast AM60B magnesium alloy*, Fatigue Fract Eng Mater Struct, **25**, pp. 45–56, 2002.
6. MOHD S., MUTOH Y., OTSUKA Y., MIYASHITA Y., KOIKE T., SUZUKI T., *Scatter analysis of fatigue life and pore size data of die-cast AM60B magnesium alloy*, Eng Failure Analysis, **22**, pp. 64–72, 2012.
7. SONSINO C.M., DIETERICH K., *Fatigue design with cast magnesium alloys under constant and variable amplitude loading*, International Journal of Fatigue, **28**, pp. 183–193, 2006.
8. LI Z., WANG Q., LUO A.A., FU P., PENG L., *Fatigue strength dependence on the ultimate tensile strength and hardness in magnesium alloys*, International Journal of Fatigue, **80**, pp. 468–476, 2015.
9. LI Z., WANG Q., LUO A. A., PENG L., ZHANG P., *Fatigue behavior and life prediction of cast magnesium alloys*, Materials Science & Engineering A, **647**, pp. 113–126, 2015.
10. KARR U., SCHÖNBAUER B.M., MAYER H., *Near-threshold fatigue crack growth properties of wrought magnesium alloy AZ61 in ambient air, dry air, and vacuum*, Fatigue Fract Eng Mater Struct, **41**, pp. 1938–1947, 2018.
11. KALATEHMOLLAEI E., MAHMOUDI-ASL H., JAHED H., *An asymmetric elastic–plastic analysis of the load-controlled rotating bending test and its application in the fatigue life estimation of wrought magnesium AZ31B*, Int J Fatigue, **64**, pp. 33–41, 2014.
12. LI X., XIONG S.M., GUO Z., *Failure behavior of high pressure die casting AZ91D magnesium all*, Mater. Sci. Eng. A, **672**, pp. 216–225, 2016.
13. UEMATSU Y., KAKIUCHI T., TAMANO S., MIZUNO S., TAMADA K., *Fatigue behavior of AZ31 magnesium alloy evaluated using single crystal micro cantilever specimen*, Int J Fatigue, **93**, pp. 30–37, 2016.
14. PARK S.H., HONG S.-G., YOON J., LEE C.S., *Influence of loading direction on the anisotropic fatigue properties of rolled magnesium alloy*, Int J Fatigue, **87**, pp. 210–215, 2016.
15. WATANABE H., *Fatigue Strength Analysis of Magnesium Alloys*, Meiden Review, **168**, pp. 37–42, 2016.
16. CONSTANTINESCU D.M., MOLDOVAN P., SILLEKENS W. H., SANDU M., BOJIN D., BACIU F., D.A. APOSTOL D.A., MIRON M.C., *Static and fatigue properties of magnesium alloys used in automotive industry*, Scientific Bulletin of University of Pitesti, Automotive Series, **19**. Vol. B, 2009.
17. DALLMEIER J., DENK J., HUBER O., SAAGE H., EIGENFELD K., *A phenomenological stress–strain model for wrought magnesium alloys under elastoplastic strain-controlled variable amplitude loading*, Int J Fatigue, **80**, pp. 306–323, 2015.
18. DALLMEIER J., HUBER O., SAAGE H., EIGENFELD K., *Uniaxial cyclic deformation and fatigue behavior of AM50 magnesium alloy sheet metals under symmetric and asymmetric loadings*, Materials and Design, **70**, pp. 10–30, 2015.
19. PATEL H.A., CHEN D.L., BHOLE S.D., SADAYAPPAN K., *Low cycle fatigue behavior of a semi-solid processed AM60B magnesium alloy*, Materials and Design, **49**, pp. 456–464, 2013.

20. BEGUM S., CHEN D.L., XUB S., LUO A. A., *Low cycle fatigue properties of an extruded AZ31 magnesium alloy*, International Journal of Fatigue, **31**, pp. 726–735, 2009.
21. ALBINMOUSA J., JAHED H., LAMBERT S., *Cyclic behaviour of wrought magnesium alloy under multiaxial load*, Int J Fatigue, **33**, pp. 1127–1139, 2011.
22. CASTRO F., JIANG Y., *Fatigue life and early cracking predictions of extruded AZ31B magnesium alloy using critical plane approaches*, Int J Fatigue, **88**, pp. 236–246, 2016.
23. HAZELI K., ASKARI H., CUADRA J., STRELLER F., CARPICK R. W., ZBIB H. .M., KONTSOS A., *Microstructure-sensitive investigation of magnesium alloy fatigue*, Int J Plasticity, **68**, pp. 55–76, 2015.
24. WANG C., LUO T., YANG Y., *Low cycle fatigue behavior of the extruded AZ80 magnesium alloy under different strain amplitudes and strain rates*, Journal of Magnesium and Alloys, **4**, pp. 181–187, 2016.
25. YIN S.M., LI S.X., *Low-cycle Fatigue Behaviors of an As-extruded Mg-12%Gd-3%Y-0.5%Zr Alloy*, J. Mater. Sci., Technol., **29**, *8*, pp. 775–780, 2013.
26. SERBAN D.A., MARSAVINA L., RUSU L., NEGRU R., *Numerical study of the behavior of magnesium alloy AM50 in tensile and torsional loadings,* Arch. Appl. Mech., **89**, pp. 911–917, 2019.
27. ***Standard test methods of tension testing wrought and cast Aluminum and Magnesium Alloy products, ASTM B 557M – 02, 2002.
28. MARSAVINA L., IACOVIELLO F., PIRVULESCU D., DI COCCO V., RUSU L., *Engineering prediction of fatigue strength for AM50 magnesium alloys*, I. J. Fat., **127**, pp.10–15, 2019.
29. *** Arbeitsanweisung fur Dynamische Abstutzkrafte, 2014.